Available online at www.sciencedirect.com

ScienceDirect

Journal of Luminescence 121 (2006) 527–534

JOURNAL OF LUMINESCENCE

www.elsevier.com/locate/jlumin

Doping effects in nanostructured cadmium tungstate scintillation films

Huamei Shang[a], Ying Wang[a], Brian Milbrath[b], Mary Bliss[b], Guozhong Cao[a,*]

[a]*Department of Materials Science and Engineering, University of Washington, 302M Roberts Hall, Seattle, WA 98195-2120, USA*
[b]*Pacific Northwest National Laboratory, Richland, WA 99352, USA*

Received 8 August 2005; received in revised form 28 November 2005; accepted 20 December 2005
Available online 24 January 2006

Abstract

This paper reports experimental study on the development of cadmium tungstate scintillator material in the form of nanocrystal films through controlled sol–gel processing and pre-designed doping. We chose cadmium tungstate as a base material for doping and nanostructure development due to its excellent inherent photoluminescence (PL) property, and chemical and thermal stability including non-hydroscopicity. Experimental results revealed that doping with Li^+, B^{3+} and Bi^{3+} resulted in appreciably reduced grain size and increased density leading to enhanced optical transmittance. Further analyses indicated that PL output changed significantly with the introduction of dopants. The relationships between doping, microstructure, and PL were discussed.

PACS: 14.20.Dh

Keywords: Cadmium tungstate; Scintillator; Sol–gel processing; Doping; Photoluminescence

1. Introduction

Among scintillating materials, cadmium tungstate ($CdWO_4$, CWO) is a high-density (7.9 g/cm^3), high-Z (atomic number) scintillator with a relatively large light yield. Due to high light output, low intrinsic background and afterglow, CWO is widely used in spectrometry and radiometry of radionuclides in extra-low activities, especially used for computer tomography (CT) [1]. Because of its capability of radiation capture, CWO has also been actively studied for applications in X-ray, γ-ray, and neutron detection [2]. Most studies and applications of CWO have been focused on high-quality single crystals grown by Czochralski method [3]; however, single crystals are expensive to grow and difficult to be integrated into microdevice fabrication process. Therefore,

---

[*] Corresponding author. Tel.: +1 206 616 9084; fax: +1 206 543 3100.
E-mail address: gzcao@u.washington.edu (G. Cao).

0022-2313/$ - see front matter © 2006 Elsevier B.V. All rights reserved.
doi:10.1016/j.jlumin.2005.12.048

polycrystalline CWO powders and films have also been reported to be made by sol–gel processing [4], pulsed laser deposition [5], spray pyrolysis [6], hydrothermal [7], polymer-controlled crystallization [8], and liquid epitaxy [9]. Among these methods, sol–gel processing is a promising candidate to make CWO powders and films and offering several unique advantages: stoichiometric composition with molecular level homogeneity for multi-component systems and low processing temperature. The unique advantages mentioned above make the sol–gel processing particularly useful or the only choice for the formation of dense polycrystalline complex oxides that decompose at elevated temperatures or consist of highly volatile constituent elements such as CdO in CWO [10]. Moderate sintering temperatures will also preserve nanosized particles, since grain growth becomes predominant only at high temperatures.

Due to poor wettability of CWO sol on substrates and low sinterability of sol–gel-derived CWO films, the ability of obtaining full densification and optical transparency in CWO films remains a great challenge [4]. Doping has been proven an effective approach to improve the sinterability to achieve a higher density and/or reduce the sintering temperature in many oxide systems [11]. Doping has also been demonstrated as an effective way to modify and/or improve various physical properties of various materials [12]. Generally, ternary tungstates are excellent light emitters [13]; however, they are also good hosts for impurities since there are two distinct constituents [14]. As a result, to distinguish between intrinsic optical properties and impurities-related behaviors is always confusing to people since their effects exist in the CWO system at the same time. With the research of intended doping, the difference between them can be distinguished easily. Doping in CWO and other tungstates single crystals has been investigated widely. The different types of ions such as uni-valence ions (Na^+, Cs^+) [15,16], di-valence ions (Co^{2+}, Pb^{2+}) [15,17,18], tri-valence ions (Bi^{3+}, Sm^{3+}) [15,19,20], and some other high-valence ions (Si^{4+}, Nb^{5+}, Mo^{6+}) [14,15] were found to have different effects on the luminescence property of CWO. However, the detailed mechanisms of doping are still not very clear. Therefore, with solution-based sol–gel processing, it is easier to dope impurity ions in CWO system and control the exact concentration of impurities. Moreover, since the low temperature sintering used in sol–gel processing, the evaporation of components will be decreased greatly compared with that of single-crystal growth processing, especially for volatile elements such as cadmium.

In this paper doping serves two purposes: (1) promotion of full densification at relatively low temperatures, and (2) introduction of elements with large γ-ray and neutron capture cross section for improved γ-ray and neutron detection efficiency. Although CWO is known as a self-activated scintillation crystal no luminescent and neutron-sensitive elements are required for neutron scintillation. However, CWO has relatively low neutron detection sensitivity. Low scintillation efficiency would effectively render the CWO films practically useless due to its small quantity of material. In this study, three oxides are chosen for doping in CWO films. ^{10}B and ^{6}Li are introduced to CWO films for enhancing the ability of neutron capture and for promoting densification. Both ^{10}B and ^{6}Li are known to have large neutron capture cross section and have been widely used in neutron detection scintillators [21,22]. Boron oxide, with a melting point of 450 °C, has been widely used to promote densification of many oxide ceramics through either forming a eutectic liquid with a low melting temperature or enhancing the diffusivity [23]. Lithium oxide is rarely used as sintering additive for other oxides; however, lithium is known to have a high solid-state diffusivity and good neutron sensitivity [1,24]. In addition to neutron sensitive elements, another oxide, Bi_2O_3, is also introduced to CWO films as a sintering additive [19]. Bi_2O_3 has a melting temperature of 820 °C and often form eutectic liquid with other oxides, and thus is commonly used as sintering additive [25,26]. In this paper, doping effects on grain size, porosity, resultant optical transmittance, and luminescence property of CWO films were investigated and discussed.

2. Experimental

The following sol–gel processing was developed and applied for the fabrication of CWO films and powders. First, 5 g tungsten oxychloride ($WOCl_4$, Aldrich) was dissolved in 85 ml isopropanol ($(CH_3)_2CHOH$) and kept stirring for 24 h at room temperature to get clear solution of tungsten isopropanol ($WO(OCH(CH3)_2)_4$). The following reaction was expected to occur [27]:

$$WOCl_4 + 4(CH_3)_2CHOH \rightarrow WO(OCH(CH3)_2)_4 + 4HCl. \quad (1)$$

Here isopropanol was chosen because it is an alcohol with bulkier chain which can slow down the hydrolysis of tungsten precursor since tungsten precursors are always sensitive to water. Then 5 ml of the above tungsten solution was taken and 0.75 ml pentanedione ($CH_3COCH_2COCH_3$, Aldrich), which works as a chelating agent to further reduce the reactivity of the above formed tungsten alkoxide precursor, was added. After stirred for 1 h, a stochiometrically equivalent amount of cadmium nitrate ($Cd(NO_3)_2 \cdot 4H_2O$, Aldrich) was dissolved into the tungsten isopropanol solution to produce a solution with a Cd/W molar ratio of 1: 1. Such a mixture was kept stirring at 350 rpm at room temperature for 1 h to allow hydrolysis and condensation reactions proceed with the crystal water in hydrated cadmium nitrate. More water is expected to be taken from the ambient by the precursor solution. The resultant sol was clear with yellow color and has a pH of ~2, and has a gelation time of ~60 days at room temperature.

Dopants were added into the above-prepared CWO sols and the doping level was controlled in the range between 0.5 and 10 atm%. However, more detailed study was carried out on the 3 and 10 atm% doping. Lithium perchlorate ($LiClO_4$, anhydrous, Alfa Aesar), trimethyl borate ($B(OCH_3)_3$, Aldrich), and bismuth acetate ($Bi_2(CH_3COO)_3$, anhydrous, Aldrich) were used to form doped CWO films and powders and doped samples are referred to as CWO:Li, CWO:B and CWO:Bi, respectively. The sols were stirred for 1 h after the addition of dopant precursors, and the resultant sols were aged at room temperature for 2 days. The doped sols were clear with yellow color, and the gelation time was found to be 65 days, a little longer than the pure CWO sol.

CWO films were made by spin-coating corresponding sol on glass substrates at a speed of 2000 rpm. Powders were obtained by allowing the sols to gel on a Petri dish at 110 °C. The films and powders were sintered at 500 °C for 1 and 4 h, respectively. During the ramping, the temperature was held at 350 °C for 1 h to remove the residual organic groups. Fig. 1 is a flow chart schematically showing the sol–gel processing and sintering conditions for the fabrication of CWO films and powders.

CWO powders and films were characterized by X-ray diffractometer (XRD, PW 1820, Phillips) and scanning electron microscope (SEM, JSM

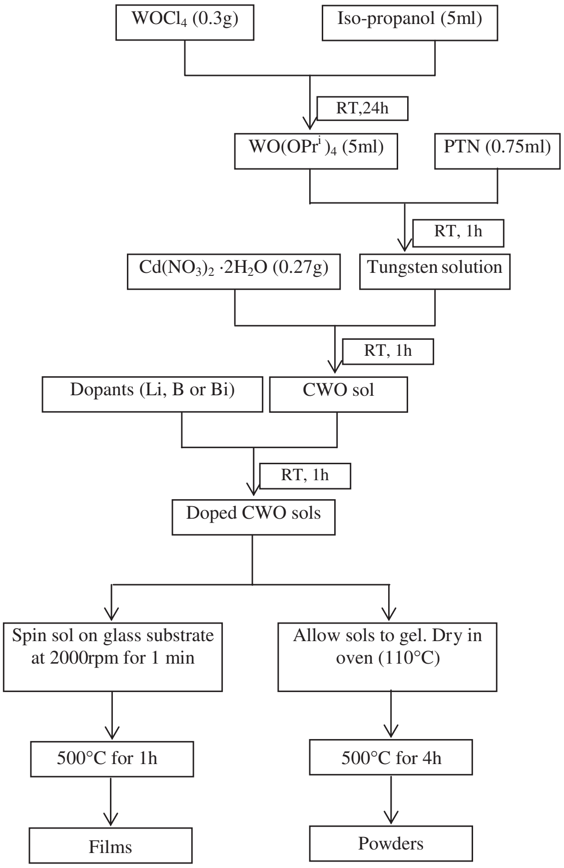

Fig. 1. Flow chart of sol–gel processing for CWO and doped CWO scintillator films and powders.

5200, JEOL). The optical transmittance and absorbance was measured by PE UV spectrophotometer. The photoluminescence (PL) spectra were obtained with an Oriel Instaspec IV charge-coupled device camera using a mercury lamp for excitation. All the films used for PL test was 1 × 1 in, and the excitation wavelength for PL was 298 nm.

3. Results and discussion

XRD spectra of pure and doped CWO (10 atm%) powders were shown in Fig. 2. In addition to the peaks identified to belong to CWO, there exist some extra peaks in all the doped samples. By comparing them with standard tungsten oxide diffraction peaks the extra peaks correspond to WO_3 phase (the peaks marked with *). There are several possible explanations on that. One is that it might be caused by the evaporation of cadmium oxide during sintering since cadmium oxide is very volatile, and that resulted in excess WO_3 or deficient CdO in the CWO samples. Second possibility is that bismuth, boron, and lithium ions substitute tungsten ions in CWO lattice, repelling WO_3. But such substitution is less likely since such replacement will cause the formation of significant quantity of oxygen vacancies to maintain the electroneutrality. Cadmium tungstate has the lower symmetry structure of wolframite, which is in the monoclinic class with one axis not orthogonal to the other two. In this structure, each tungsten atom is surrounded by six near-oxygen sites in approximately octahedral coordination. CWO is an excellent host for impurity ions, so when dopants such as Li^+, B^{3+}, and Bi^{3+}, are introduced into CWO crystal lattice, there are two possible sites they can enter: substitutional site and interstitial site. However, it is known that package of ABO_4-type crystal lattice practically does not permit the interstitial arrangement of impurity ions [28]. Therefore, the defects formed with doping ions in CWO lattice should be substitutional, and the doping ions can replace both Cd^{2+} and W^{6+} ions that both lie in the octahedral centers of oxygen O^{2-} ions depending on the radii and charges of those dopant ions [19]. There are two possible structures of doped CWO crystal lattice based on the structure of CWO lattice determined by Morell [29]. Although it has been widely suggested that impurity ions will substitute cadmium site in doped CWO crystals [9,17], the radii of these ions ($R_{\mathrm{Cd}} = 0.97\,\text{Å}$, $R_{\mathrm{W}} = 0.62\,\text{Å}$, $R_{\mathrm{Bi}} = 1.03\,\text{Å}$, $R_{\mathrm{Li}} = 0.76\,\text{Å}$ and $R_{\mathrm{B}} = 0.23\,\text{Å}$, all with a coordination number of 6 except for boron with coordination number of 4) vary significantly [30]. Obviously, preferential substitution at tungsten site is hard to justify, particularly when the ionic radius is concerned, though partial substitution at a relatively low concentration might be possible. Therefore, substitution at cadmium site is most possible in lithium- and bismuth-doped CWO. However, for B^{3+}-doped sample, since the radius of B^{3+} is so small compared to both Cd^{2+} and W^{6+} ions, there is another possibility. Boron cation has an ionic radius of 0.23 Å and can only have a coordination number of 4; it is very likely that boron will not substitute either cadmium or tungsten to enter CWO crystal lattice. Instead, boron may preferentially react with CdO to form a grain boundary or secondary phase (either amorphous or crystalline), leaving extra WO_3 as another phase in the

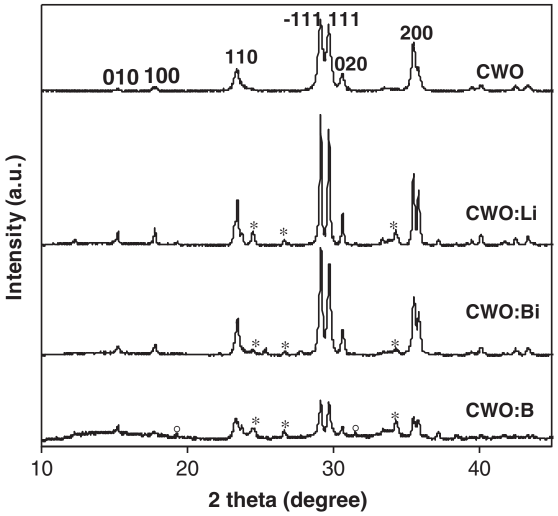

Fig. 2. XRD spectra of CWO, CWO: Li, CWO: Bi, and CWO: B polycrystalline powders. The doping concentration in all doped films is 10 atm%. The extra peaks marked with * are WO_3, marked with ° are $Cd_3B_4O_9$.

sample. The extra peaks in CWO:B powder are possible indications of the formation of such a grain boundary or secondary phase—$Cd_3B_4O_9$ (marked with ° in Fig. 2). The doping process in powders and sol–gels is complex since various phases can be easily formed. Further experiments are required and underway to clarify and explain the XRD results.

SEM analyses in Fig. 3 revealed that addition of various dopants into CWO resulted in appreciably enhanced densification with all other processing conditions kept the same. In the present study, 10 atm% lithium oxide, boron oxide, and bismuth oxide are introduced as sintering additives to promote the densification of cadmium tungstate films, though both lithium and boron are also used as neutron-sensitive elements. When sintering additives form a liquid phase and homogeneously dispersed at grain boundaries, it is expected to promote densification at relatively low sintering temperature by introducing liquid phase as alternate mass transport media [31]. On the other hand, the presence of such grain boundary phase is anticipated to prevent excessive and abnormal grain growth by setting a diffusion barrier between adjacent grains and increasing the diffusion distance from one grain to another. As a result, grain growth will be significantly suppressed while an appreciable densification can be achieved at relatively low sintering temperature. The above discussion can be best exemplified by boron- and lithium-doped cadmium tungstate films. With the addition of boron and bismuth, no appreciable grain growth is observable; the particle size of CWO is estimated to be ~200 nm, and boron- and bismuth-doped films have even smaller particle size. The density of these two doped films has been significantly enhanced under the same sintering

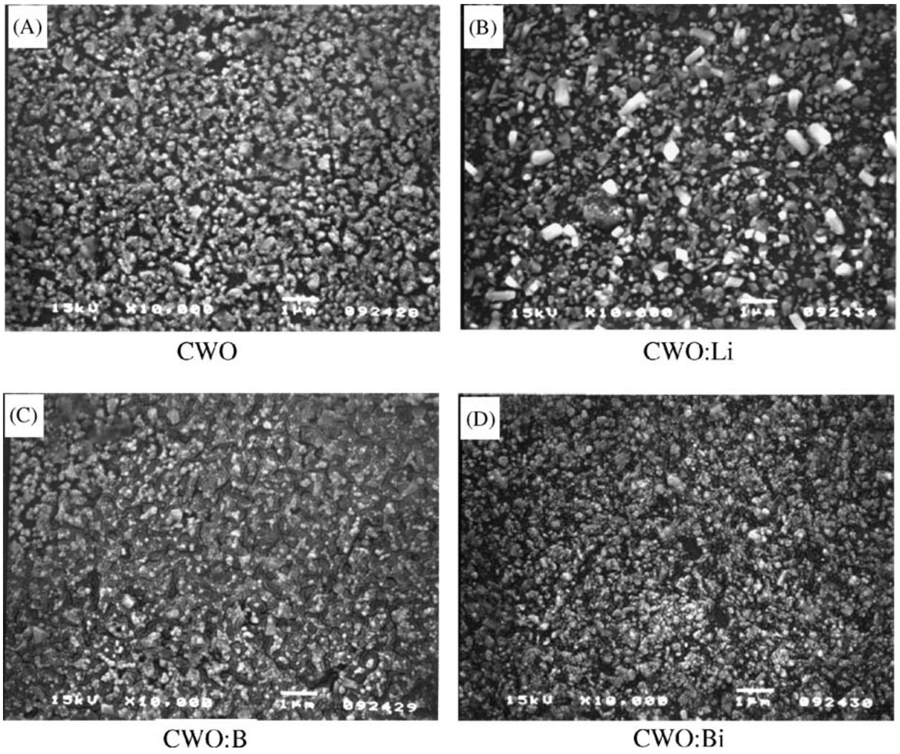

CWO

CWO:Li

CWO:B

CWO:Bi

Fig. 3. SEM micrographs showing the morphologies and grain sizes of CWO with and without doping. The doping concentration in all doped films is 10 atm%. A is CWO, B is CWO: Li, C is CWO: B, and D is CWO: Bi. The morphologies of CWO, CWO: B, and CWO: Bi are quite similar, and they all consist of spherical particles but different particle size and pore size, however, the morphology of CWO: Li is the packing of well-faceted platelets.

conditions, as compared with undoped CWO films (Fig. 3A, C and D). The introduction of lithium has also seen the appreciable influences on the morphology of the CWO grains. Most notable change is that the grain facets are very well developed in this sample which also results in enhanced density. The qualitative difference in film densities by comparison of SEM images is supported by more precise measurement of the bulk density of the samples that were by powder–pellet sintering. Four pellets of CWO, CWO:Li, CWO:B, and CWO:Bi, all with a doping level of 10 atm%, were pressed and sintered under identical conditions—500 °C for 4 h. The densities were estimated to be 4.52 g/cm^3 for CWO, 4.89 g/cm^3 for CWO:Li, 4.66 g/cm^3 for CWO:B, and 4.65 g/cm^3 for CWO:Bi, respectively. The nominal increases of density by doping are: CWO:Li = 8.2%, CWO:B = 3.2%, and CWO:Bi = 2.8%. It should be noted that the powder pellets have relative low density and sol–gel-derived films possess higher density due to a better packing induced by capillary force during the removal of solvent. However the general tendency of change in density is similar and comparable.

Fig. 4 shows the absorption spectra of doped and undoped CWO films (10 atm%) in the wavelength region from 230 to 700 nm. The most notable difference is the shift of absorption edge. CWO films doped with boron, lithium, and bismuth have a red shift in their absorption edges. So it is indicative that the presence of the doping elements has notable effect on the crystallinity or band structure of CWO by forming substitutional defects and/or oxygen vacancies. Fig. 4 also shows that doped CWO films have higher optical transmittance throughout the entire visible light spectrum than that of CWO film. The enhancement in optical transmittance at shorter wavelengths is more pronounced than that in the longer wavelength. Considering the fact that all films have the similar thickness (around 400 nm) and grain size, the enhanced transmittance in doped films is likely attributable to the difference in density or porosity. All doped films with significantly higher density possess far less pores or lower porosity; consequently there will be much less scattering caused by the pores, resulting in a much enhanced optical transmittance.

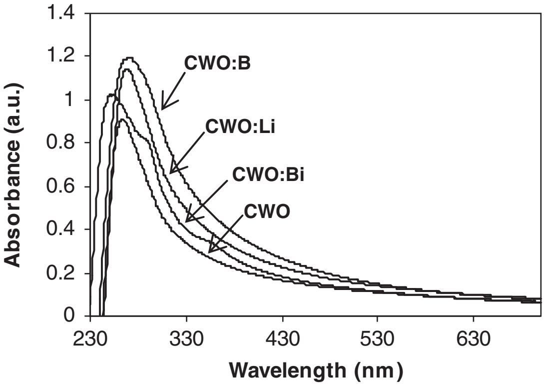

Fig. 4. Absorbance spectra of CWO film and doped films. The doping concentration in all doped films is 10 atm%. The transmittance increase in all doped films compared to pure CWO film, and absorbance decrease in the order of CWO: B, CWO: Li, CWO: Bi and CWO.

Fig. 5 is the comparison of PL spectra of CWO, CWO:Li, CWO:B, and CWO:Bi films excited by a 298 nm UV light. Bismuth doping resulted in total loss of characteristic PL of CWO at 480 nm. However, the characteristic PL is retained in both lithium- and boron-doped films, albeit the PL intensity varies significantly. Boron doping resulted in a reduction of more than 60% in PL intensity. Lithium doping is more complicated; PL increases at a doping level of 3 atm% (Fig. 5A), whereas decreases at 10 atm% (Fig. 5B). It is known that the introduction of dopants to tungstate compounds would impair their characteristic PL, except lead in CaWO$_4$, which can enhance the PL of the host as long as the content of dopants does not exceed a certain percent [32]. The loss of characteristic PL with bismuth doping or the reduction of PL intensity with boron doping may well be attributed to the defects introduced to the CWO crystal lattice and the second phase stay in the grain boundary. When the trivalent ions of Bi^{3+} enter Cd^{2+} sites, some cadmium vacancies may form in CWO lattice to keep charge neutrality. Such point defects likely result in extra defect energy states, leading to the PL in a longer wavelength, but reducing the intrinsic emission of CWO at 480 nm. For better comparison, PL spectra are normalized to bring their peaks to the

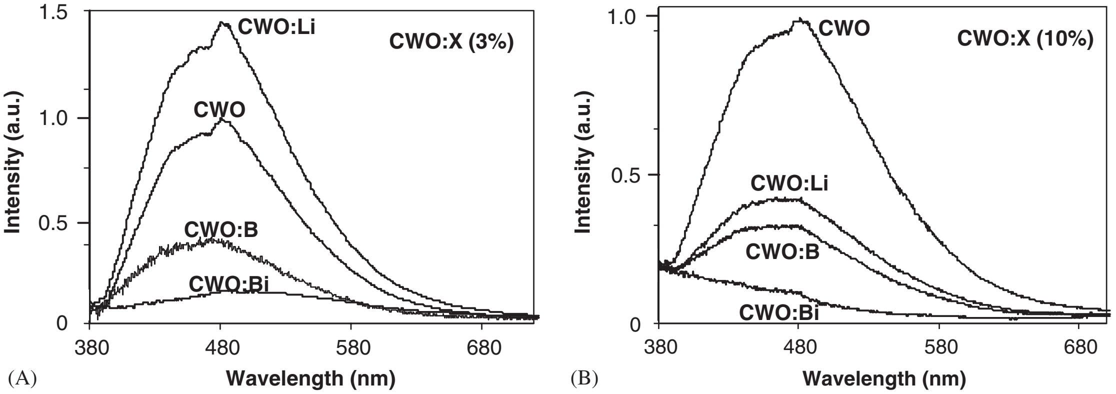

Fig. 5. Photoluminescence spectra of CWO and doped films. The content of dopants in A is 3 atm%, and the content of dopants in B is 10 atm%. The excitation wavelength is 298 nm.

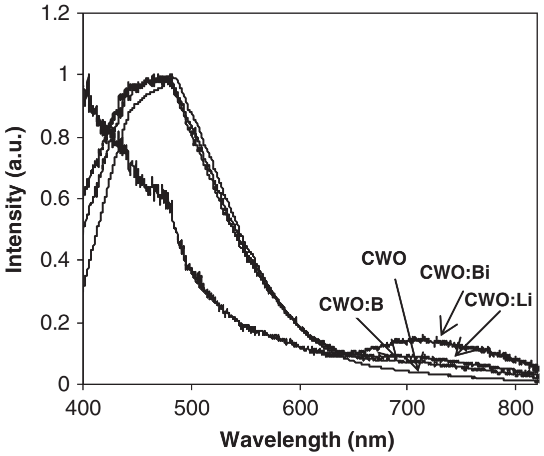

Fig. 6. Normalized photoluminescence spectra, some extra luminescence peak found in long wavelength. The doping concentration is 10 atm%, and excitation wavelength is 298 nm.

same height (as shown in Fig. 6). The broadening of the characteristic PL peak due to the introduction of doping elements may be attributed to the inhomogeneity in local atomic environment. The peak in a longer wavelength around 700 nm in 10 atm% bismuth-doped CWO may be attributable to transitions within the Bi^{3+} ions, although combined electron paramagnetic resonance and optical study suggested the emission caused by oxygen vacancies should be a broad yellow emission peaking near 550 nm at 296 K [19,33]. Influence of lithium doping is complex. On one hand, substitution of Cd^{2+} by Li^{+} requires the formation of oxygen vacancies to maintain the electroneutrality, and thus leads to quench of the characteristic PL. Considering the difference in valence states, the quench of the characteristic PL would be significant, even at a relatively low doping concentration. On the other hand, the presence of lithium oxide during the processing of CWO films resulted in a much improved crystallinity as suggested by well-defined crystal facets shown in Fig. 3B. The enhanced intensity of PL may well suggest that there is indeed a significant improvement in CWO crystallinity with the addition of lithium oxide.

4. Conclusions

CWO films and powders were made by sol–gel processing with Li^{+}, B^{3+}, or Bi^{3+} doping. All the films are homogeneous and crack-free, and regardless of the presence of doping ions, XRD and SEM analyses revealed that polycrystalline CWO phase was formed with an average grain size up to 200 nm. Doping ions have effectively promoted densification at a relatively low temperature without any detectable grain growth, leading to enhanced optical transmittance. All the films showed intrinsic photoluminescence (PL) of CWO around 480 nm when excited by UV light of

298 nm. Further analyses indicated that PL output changed significantly with the types and concentrations of dopants. Lithium doping can enhance the PL of CWO at low concentrations, and quench it at high concentrations. Boron-doped films had lower luminescence both at high and low concentrations. The characteristic PL peak disappeared with bismuth doping, but resulted in a broad yellow emission.

Acknowledgments

The authors would like to acknowledge the financial support from Pacific Northwest National Laboratories. MHS and YW acknowledge the Joint Institute for Nanoscience (JIN) Fellowships and the Ford Motor Company Fellowships. The authors would also acknowledge Prof. Alex Jen, Dr. Yuhua Niu and Dr. Michelle Liu for their great help for PL measurements.

References

[1] L. Nagornaya, G. Onyshchenko, E. Pirogov, N. Starzhinskiy, I. Tupitsyna, V. Ryzhikov, Y. Galich, Y. Vostretsov, S. Galkin, E. Voronkin, Nucl. Instrum. Methods A 537 (2005) 163.

[2] V. Ryzhikov, L. Nagornaya, V. Volkov, V. Chernikov, O. Zelenskaya, Nucl. Instrum. Methods A 486 (2002) 156.

[3] L. Nagornaya, S. Burachas, Y. Vostretsov, V. Martynov, V. Ryzhikov, J. Cryst. Growth 198–199 (1999) 877.

[4] K. Lennstrom, S.J. Limmer, G.Z. Cao, Thin Solid Films 434 (2003) 55.

[5] K. Tanaka, N. Shirai, I. Sugiyama, R. Nakata, Nucl. Instrum. Methods B 121 (1997) 404.

[6] Z.D. Lou, J.H. Hao, M. Cocivera, J. Lumin. 99 (2002) 349.

[7] H.W. Liao, Y.F. Wang, X.M. Liu, Y.D. Li, Y.T. Qian, Chem. Mater. 12 (2000) 2820.

[8] S.H. Yu, M. Antonietti, H. Cölfen, M. Giersig, Angew. Chem. Int. Ed. 41 (2002) 2356.

[9] Y.J. Xiong, Y. Xie, Z.Q. Li, X.X. Li, S.M. Gao, Chem. Eur. J. 10 (2004) 654.

[10] A. Montenero, M. Canali, G. Gnappi, D. Bersani, P.P. Lottici, P. Nunziante, E. Traversa, Appl. Organomet. Chem. 11 (1997) 137.

[11] Y. Wu, C.P. Nguyen, S. Seraji, M.J. Forbess, T.P. Chou, G.Z. Cao, J. Am. Ceram. Soc. 84 (2001) 2882.

[12] Y. Wu, G.Z. Cao, Appl. Phys. Lett. 75 (1999) 2650.

[13] G. Blasse, B.C. Grabmaier, Luminescent Materials, Springer, Berlin, 1994.

[14] N.Y. Garces, M.M. Chirila, H.J. Murphy, J.W. Foise, E.A. Thomas, C. Wicks, K. Grencewicz, L.E. Halliburton, N.C. Giles, J. Phys. Chem. Solids 64 (2003) 1195.

[15] M. Kobayashi, Y. Usuki, M. Ishii, M. Itoh, Radiat. Meas. 38 (2004) 375.

[16] V. Tale, I. Tale, L.L. Nagornaya, Radiat. Eff. Defects Solids 134 (1995) 477.

[17] U. Rogulis, Radiat. Meas. 29 (1998) 287.

[18] Y. Zorenko, L. Limarenko, I. Konstankevych, M. Pashkovsky, Z. Moroz, I. Solsky, B. Grinev, V. Nekrasov, Y. Borodenko, Semicond. Phys. Quant. Ele. Optele. 3 (2000) 207.

[19] H.J. Murphy, K.T. Stevens, N.Y. Garces, M. Moldovan, N.C. Giles, L.E. Halliburton, Radiat. Eff. Defects Solids 149 (1999) 273.

[20] O. Chukovaa, S. Nedilko, Z. Moroz, M. Pashkovskyi, J. Lumin. 102–103 (2003) 498.

[21] H. Pomerance, Phys. Rev. 83 (1951) 641.

[22] M. Bliss, R.A. Craig, D.S. Sunberg, M.J. Weber, Ceram. Trans. 67 (1996) 109.

[23] C.F. Yang, C.M. Cheng, Ceram. Int. 25 (1999) 383.

[24] B.M. Suleiman, A. Lundén, E. Karawacki, Solid State Ionics 136–137 (2000) 325.

[25] S. Geller, H.J. Williams, G.P. Espinosa, R.C. Sherwood, M.A. Gilleo, Appl. Phys. Lett. 3 (1963) 21.

[26] Y.Y. Song, S.C. Yu, W.T. Kim, J.R. Park, T.H. Kim, J. Magn. Magn. Mater. 177–181 (1998) 257.

[27] O.J. Klejnot, Inorg. Chem. 4 (1965) 1668.

[28] S.G. Nedilko, M. Diab, L.M. Limarenko, Z.T. Moroz, M.V. Pashkovskyi, Ukr. Phys. J. 42 (1997) 415.

[29] D.J. Morell, J.S. Cantrell, L.L.Y. Chang, J. Am. Ceram. Soc. 63 (1980) 261.

[30] D.R. Lide, (Ed.), Handbook of Chemistry and Physics, 84th ed., CRC Press, LLC, 2003.

[31] M.N. Rahaman, Ceramic Processing and Sintering, Marcel Dekker, Inc., New York, 1995.

[32] P. Pringsheim, Fluorescence and Phosphorescence, Interscience Publishers, Ins., New York, 1963.

[33] M.M. Chirila, K.T. Stevens, H.J. Murphy, N.C. Giles, J. Phys. Chem. Solids 61 (2000) 675.